Cold-target recoil-ion momentum spectroscopy studies of capture from atomic and molecular hydrogen by O^{8+} and Ar^{8+}

E. Edgu-Fry,* A. Wech, J. Stuhlman, T. G. Lee,† C. D. Lin, and C. L. Cocke‡
J. R. Macdonald Laboratory, Department of Physics, Kansas, State University, Manhattan, Kansas 66506, USA
(Received 12 January 2004; published 19 May 2004)

We have used cold-target recoil-ion momentum spectroscopy to study electron capture from atomic and molecular hydrogen targets by slow ($0.3 < v < 0.95$ a.u.) O^{8+} and Ar^{8+} ions. For the atomic hydrogen target, we have performed coupled-channel calculations using an atomic orbital expansion to compare to the experimental results. The *Q*-value spectra show strong populations of both $n=5$ and $n=6$ states on the projectile, with a tendency for increasing the population of high-angular momentum states for higher projectile velocity. A strong population of $n=6$ is found, a result not previously reported but in good agreement with the present calculations.

DOI: 10.1103/PhysRevA.69.052714 PACS number(s): 34.70.+e, 34.50.Fa

I. INTRODUCTION

The subject of electron capture from neutral molecules has been heavily studied over the past two decades [1–5]. It is well understood that the process takes place via a long-range over-barrier transfer. The data include total and partial cross sections, *Q*-value distributions obtained through translational energy spectroscopy, and projectile angular distribution measurements. Here *Q* is the change in electronic energy in the transfer, with positive *Q* corresponding to an exoergic reaction. The determination of *Q* reveals the states into which the capture proceeds. In recent years it has become possible to obtain both the *Q* value and angular distributions simultaneously in high resolution and over a wide range of projectile velocities using cold-target recoil-ion momentum spectroscopy (COLTRIMS) [6–12]. Several theoretical models have been employed to account quantitatively for both the *Q* value and angular distributions. One of the most successful theoretical approaches has been the coupled-channel atomic orbital expansion method. This approach has been able to account nearly exactly for experimental results of this nature for a range of targets and for projectile velocities up to about 1 a.u. [13–16].

As the comprehensive nature of the data has increased, the calculations have been put to more and more stringent tests, which they have generally met within the bounds of certain uncertainties inherent to the problem. One such boundary has been the necessity to model the usual multi-electron targets as one-active-electron-plus-core systems. In this article we avoid this uncertainty. We report the use of a quasicold atomic hydrogen target to carry out electron capture studies. Removing this limitation appears nearly to remove the last vestiges of disagreement between experiment and calculation.

The system we have chosen for study is the capture by 8^+ ions from atomic hydrogen. For O^{8+} on atomic hydrogen, the collision system is a true one-electron one, thus removing completely any necessity for any modeling of either projectile or target potential. Only true Coulomb potentials are involved. However, this system suffers from the problem that experimental resolution of capture to different subshells cannot be achieved with our technique. Therefore we have also studied Ar^{8+} on H. For this system, the quantum defects are sufficiently large to allow subshell separation. We pay for this improvement with the necessity to use a model potential for the projectile-electron interaction. However, since an Ar^{8+} ion appears nearly pointlike to the target for the large impact parameters at which the transfer occurs, we believe this to be an acceptable and small price.

Many previous studies have been carried out for O^{8+} and Ar^{8+} on multielectron targets. We limit our background discussion here to cases directly relevant to the present studies. Several total cross-section capture measurements by these projectiles specifically on atomic (and usually also molecular) hydrogen targets have been reported. Crandall *et al.* [17] reported cross sections by many highly charged projectiles, including Ar^{8+}, for projectile velocities typically below about 0.5 a.u. Meyer *et al.* [18] reported cross sections for O^{8+} in the 0.1–10 keV/amu range and found different energy behaviors for the two targets at the lowest energies. Can *et al.* [19] measured total cross sections for various highly charged projectiles including Ar^{8+} using a recoil-ion source in the 200–1000 eV/amu range and found very flat energy dependences. Dijkkamp *et al.* [20] measured line-emission cross sections for O^{8+} in the energy range 3–7.5 keV/amu. Hoekstra *et al.* [21–23] used line emission to study state-selective capture for O^{8+}. Among the findings was the result that, while existing calculations accounted well for the main channels, discrepancies were found for weak ones. Giese *et al.* [24] performed translational energy spectroscopy for projectiles including Ar^{8+} on atomic hydrogen at the low projectile energy of 4.36 keV. Related translational energy spectroscopy has been reported more recently by Kearns *et al.* [25] and some other relevant publications include Ref. [20]. Numerous theoretical calculations have been carried out for O^{8+} [26–31] and Ar^{8+} [32].

*Present address: Physics Division, National Institute of Technology, Gaithersburg, MD 20899, USA.
†Present address: Physics Division, Oak Ridge National Laboratory, Oak Ridge, TN 37831, USA.
‡Electronic address: cocke@phys.ksu.edu

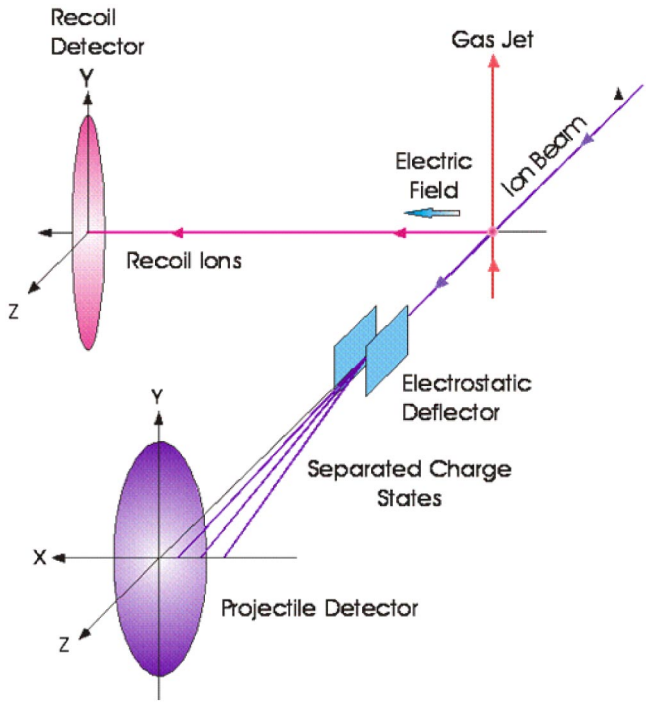

FIG. 1. (Color online) Collision schematic.

II. EXPERIMENTAL METHOD

The experiments were conducted at the KSU-CRYEBIS facility. The basic setup of the beamline and the COLTRIMS spectrometer are described in Refs. [8,12]. The major technical innovation reported here is the coupling of an atomic hydrogen target to a COLTRIMS spectrometer. A schematic is shown in Fig. 1. Briefly, the Ar^{8+} and O^{8+} beams were delivered from the KSU-Cryebis facility at acceleration voltages between 5 and 70 kV and with beam currents ranging from 2 pA (lowest energy O^{8+}) to 200 pA (highest energy Ar^{8+} beam). After collimation by a 1-mm-diam aperture, the ion beam crossed an effusive gas jet composed of a mixture of atomic and molecular hydrogen, and thereafter proceeded downstream through an electrostatic analyzer, which allowed the selection of the charge-exchanged component of the beam. These particles were detected by a position-sensitive channel-plate detector. The signal from this detector was used to start a time-to-amplitude converter. Meanwhile the singly charged hydrogen ions were propelled by a transverse electric field of typically 10 V/cm onto the face of a second position-sensitive channelplate detector. The position and time of arrival of these recoil ions was used in the usual manner to calculate the momentum of the ions at the time they emerged from the capture collision.

The atomic hydrogen target was prepared by dissociating H_2 in a microwave discharge, following the arrangement described by Paolini and Khakoo [33]. This source uses microwave radiation at 2450 MHz in a resonantly tuned Evenson cavity to dissociate the hydrogen gas. A quartz discharge tube operated within the resonant cavity, and the gas exiting the discharge was led through a 22-cm-long Teflon tube to a quartz needle. The exit of the needle, a 0.5-mm-diam canal 5 mm long, sent the gas through a 0.5 mm skimmer located 7 mm away, from which the collimated jet proceeded another 5 cm to intersect the beam. The discharge tube, the Teflon tube and the nozzle all were thoroughly cleaned to remove dust and dirt, which could enable recombination of the atomic hydrogen. They were cleaned by soaking overnight in orthophosphoric acid and washed with distilled water. They were then soaked in acid again and dried in a 100 °C oven for 2–3 hours. During pumping and venting procedures, the pressure of the discharge tube remained higher than the pressure of the chamber to avoid gas flowing back into the discharge tube. The source was tuned to deliver a reflected power measured of 1–2 W while the forward power was 50–55 W. The pressure was typically 1.2×10^{-5} Torr in the nozzle region and about 200–400 mTorr

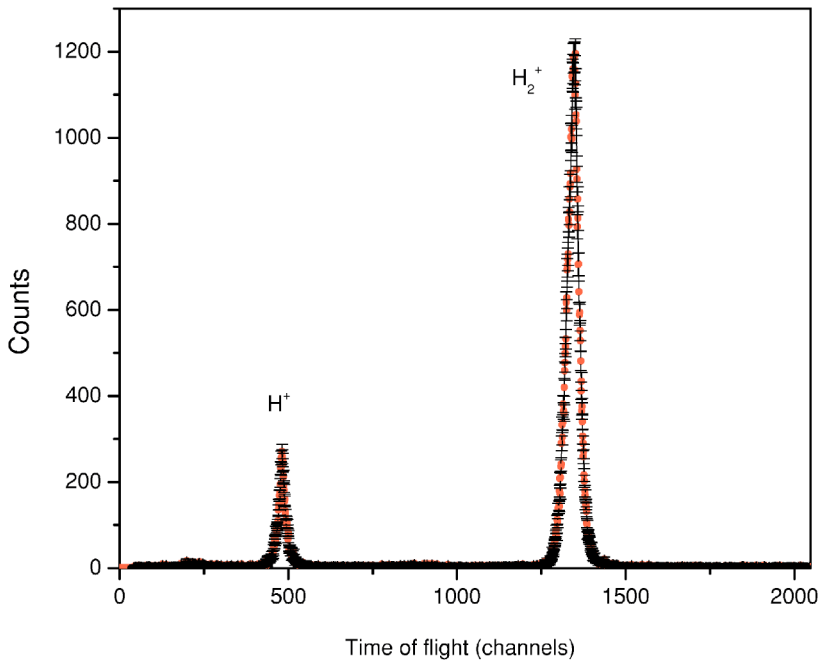

FIG. 2. (Color online) Time-of-flight spectrum for capture by O^{8+} at $v=0.96$ a.u. The H_2^+ ions come from both the jet and the background gas and can be separated further, while the H^+ ions come only from the jet.

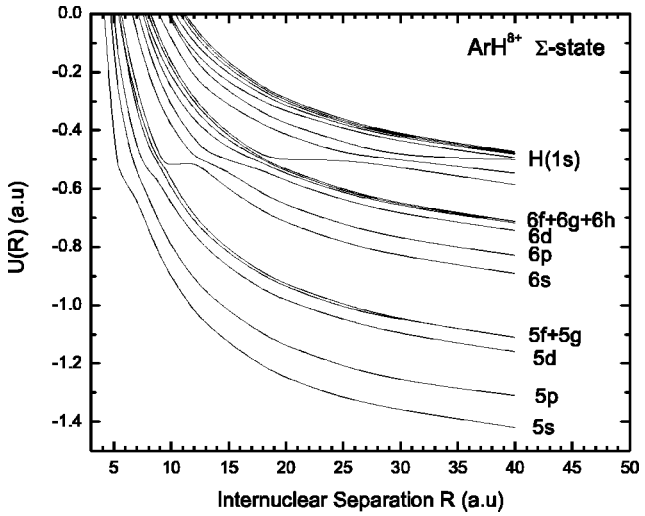

FIG. 3. MO potential curves for the ArH^{8+} molecular ion.

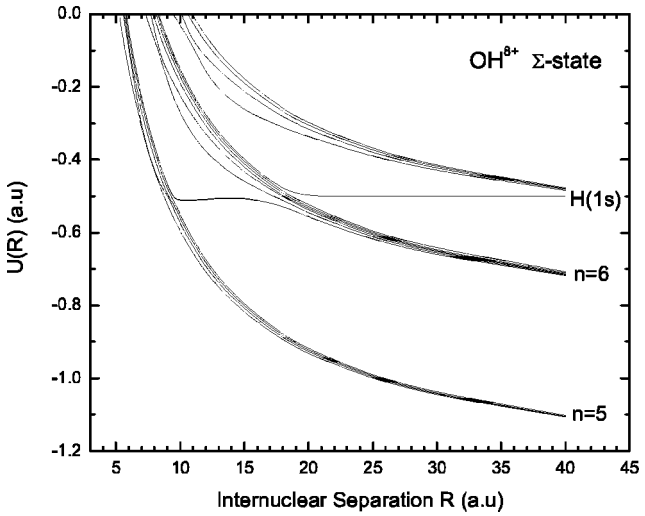

FIG. 4. MO potential curves for the OH^{8+} molecular ion.

in the discharge tube. The final dissociation fraction realized in the jet was between 25% and 50%, (see Fig. 2) indicating significant recombination in the Teflon transport tube. However, this modest dissociation fraction posed no problem for the experiment, since the separation of atomic and molecular hydrogen ions was trivially accomplished using their different times of flight. The source operated stably over days. During this time efficient operation was indicated by the deep red glow of the discharge. Occasional periods of low dissociation fraction, occurring every several hours and lasting tens of minutes, were indicated by a pale white discharge. This behavior proved easier to tolerate than to prevent. The resulting effusive-flow gas jet was composed of a mixture of atomic and molecular hydrogen. The ion beam was collimated by an aperture in the entrance to the collision chamber to 1 mm in diameter. The width of the jet in the collision area was about 3.5 mm with a density of about 10^9 atoms/cm^3.

The momentum resolution of the apparatus was limited by the momentum spread in the jet. Transverse to the gas motion, the jet is geometrically cooled by the collimators, resulting in a resolution of 0.14 a.u for atomic hydrogen in the z and x directions. Here we take z to be along the beam direction, y along the jet, and x along the direction of the extraction field. Fortunately the energy transfer axis is the z axis, and we have good resolution in this direction. The jet is not cooled in the y direction, and the resulting resolution is approximately 2 a.u. full width at half maximum for atomic hydrogen in this direction.

III. THEORETICAL MODEL

The two-center atomic orbital close-coupling (TCAOCC) method within the semiclassical formalism has been described fully in the monograph of Bransden and McDowell

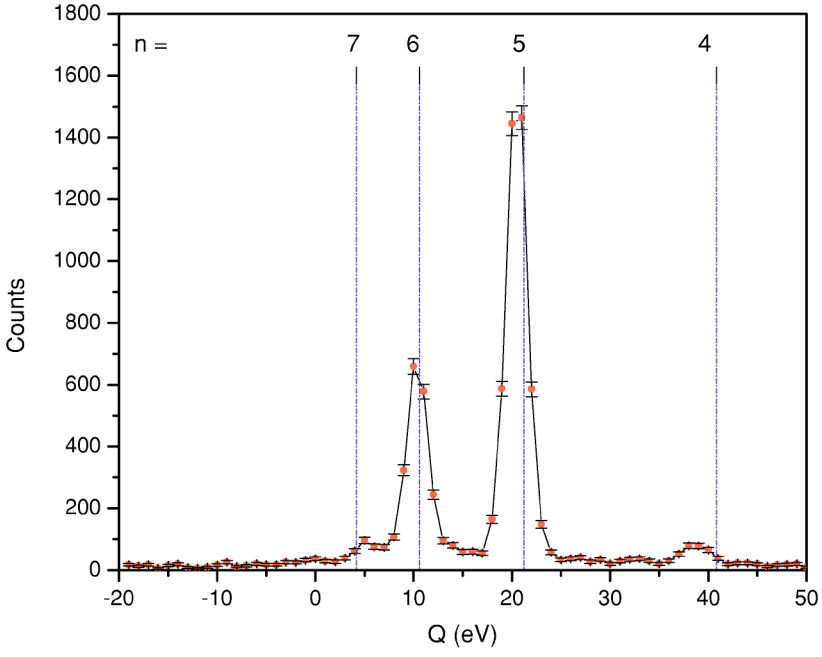

FIG. 5. (Color online) Q-value spectrum for single capture from atomic hydrogen by O^{8+} ions at $v=0.50$ a.u. The dashed lines indicate the expected locations for capture into different principal quantum numbers n on the O^{7+} product ion.

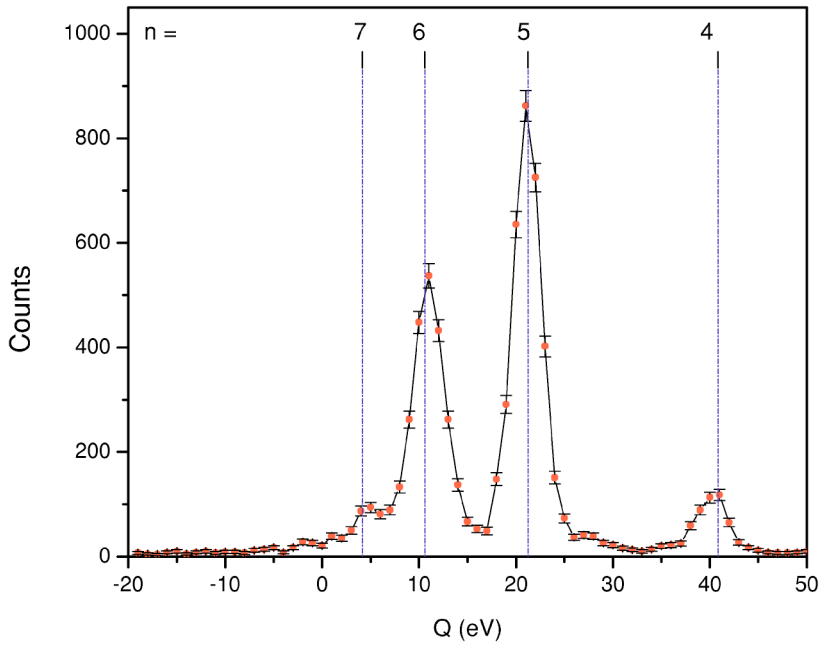

FIG. 6. (Color online) Similar to Fig. 5, but for $v=0.75$ a.u.

(1992) [13] and the review paper by Fritsch and Lin [14], and therefore the details need not be repeated here. In this section, only summaries of important features of this method will be given.

Briefly, the two center time-dependent electronic wave function that satisfies the Schrödinger equation is expanded in terms of a basis set that consists of products of atomic orbitals and an appropriate plane-wave electron translational factors. The atomic orbitals are expressed in terms of even-tempered basis functions and the method has been applied to many ion-atom collision systems at low to intermediate energies [15,16]. In the case of a $O^{8+}+H(1s)$ system, the interaction potential between the electron and the bare ion is purely Coulombic. However, for an $Ar^{8+}+H(1s)$ collision, a model potential has been used to describe the interactions between the active electron and the ionic core of Ar^{8+}. In the AOCC calculation, the Ar^{7+} is approximated as a one-electron atom, where the electron moves in a spherically symmetric potential, including Coulomb and screening interaction, from the ionic core [8]:

$$V_{\mathrm{Ar}^{7+}}(r) = -\frac{1}{r}[8 + (10 + 5.5r)e^{-5.5r}]. \tag{1}$$

The parameters in the model potential are chosen such that the experimental electronic binding energies of the first few states of interest are well reproduced. In the present TCAOCC calculations, a set of 94 states with $n=4-8$ and l

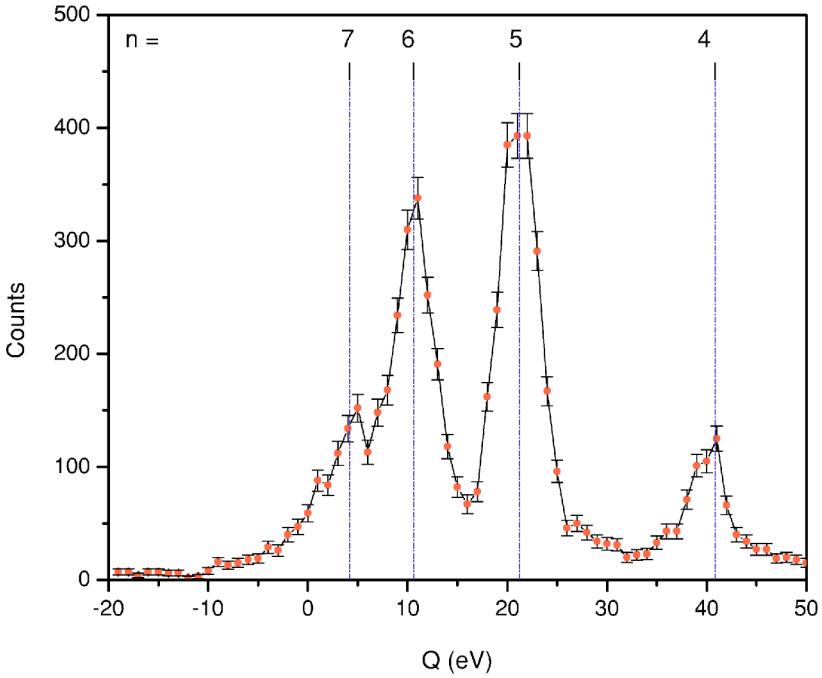

FIG. 7. (Color online) Similar to Fig. 5, but for $v=0.96$ a.u.

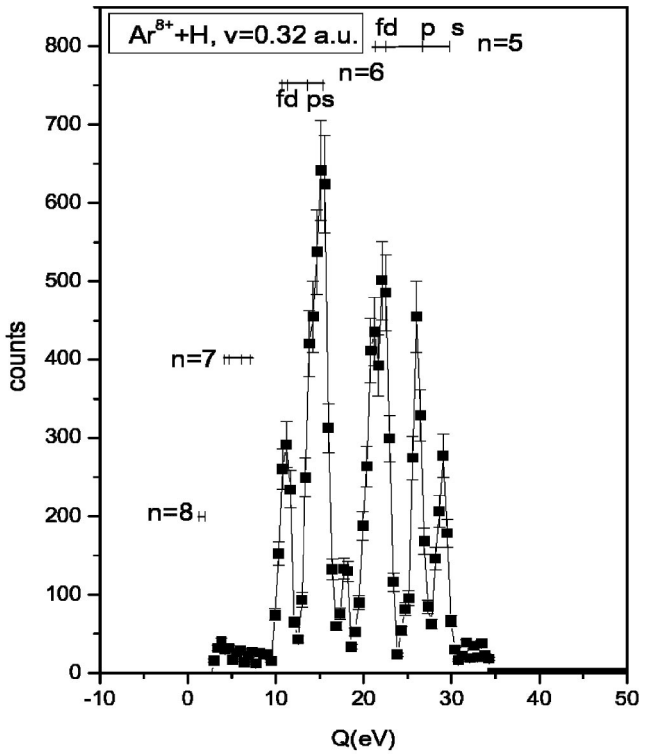

FIG. 8. Q-value spectrum for single capture from atomic hydrogen by Ar^{8+} ions at $v=0.32$ a.u. The short bars indicate expected locations for capture into different (n,l) on the Ar^{7+} product ion.

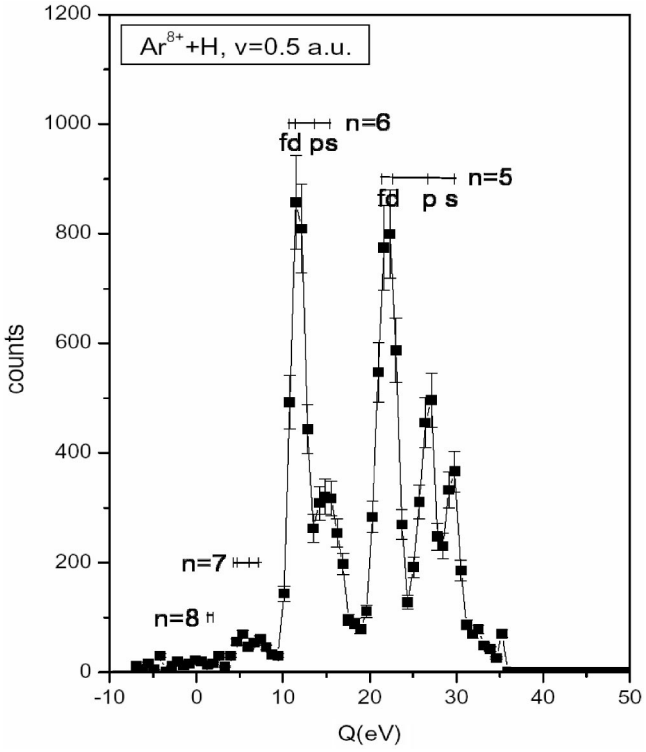

FIG. 9. Similar to Fig. 8, but for $v=0.50$ a.u.

$=0-5$ are included on the projectile centers (i.e., Ar^{8+} and O^{8+}), whereas for the target center, only H(1s) is considered. The electronic binding energies of $Ar^{7+}(nl)$ states obtained from the model are in excellent agreement with those given in the National Institute of Science and Technology (NIST) Data Center compilation [34].

In understanding the results, it is useful to have the molecular potential curves. However, in the AOCC method, such potential curves are not calculated. The molecular potential curves of ArH^{8+} and OH^{8+} were calculated separately using the Born-Oppenheimer (BO) approximation and the important Σ molecular states are shown in Fig. 3 and 4, respectively.

IV. EXPERIMENTAL RESULTS AND COMPARISON WITH THEORY

The longitudinal momentum transfer (p_{rz}) to the recoil, was converted to Q value using the relationship [8,12]

$$Q = -v\ p_{rz} - v^2/2,$$

where v is the projectile velocity and atomic units are used. The position with which a recoil with no longitudinal momentum would hit on the detector was calibrated using the resonant charge transfer reactions $p+H>H+p$ and $H_2^+ + H_2 > H_2 + H_2^+$. In principle, it might be expected that either reaction would be sufficient to determine this zero-momentum position, since the H^+ and H_2^+ ions should have the same zero. It was found, however, that these recoil ions

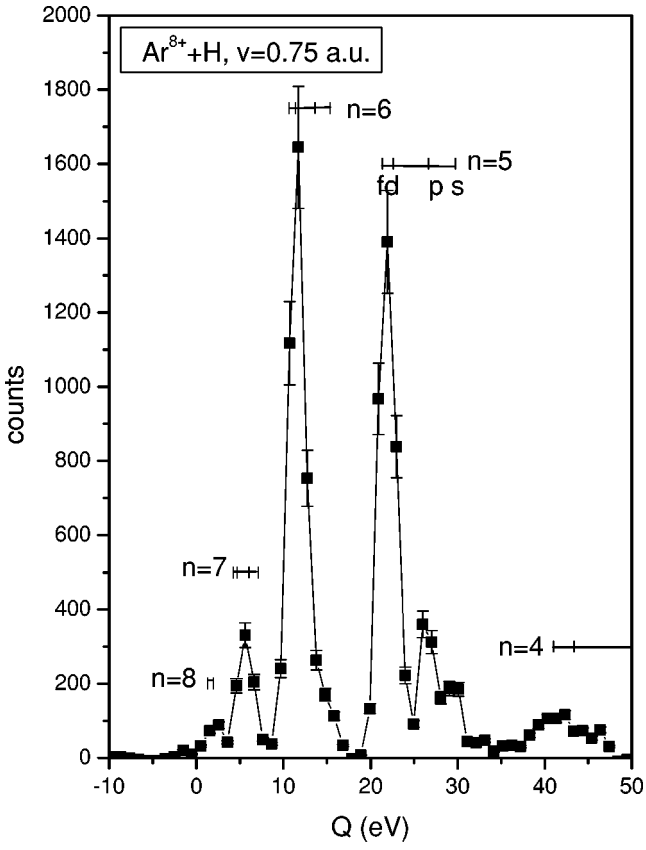

FIG. 10. Similar to Fig. 8, but for $v=0.75$ a.u.

TABLE I. Comparison of relative cross sections between theory and experiment for $Ar^{8+}+H(1s)$. These numbers are normalized to unity. The $v=0.3$ experimental data were actually taken at $v=0.32$ a.u.

v (a.u.)	σ_n	AOCC	Experiment
0.3	$5s$	0.084	0.082
	$5p$	0.194	0.145
	$5d+5f+5g$	0.443	0.301
	$\boldsymbol{n=5}$	0.721	0.531
	$6s+6p$	0.179	0.363
	$6d+6f+6g+6h$	0.0997	0.106
	$\boldsymbol{n=6}$	0.279	0.468
0.5	$5s$	0.094	0.092
	$5p$	0.190	0.165
	$5d+5f+5g$	0.368	0.297
	$\boldsymbol{n=5}$	0.650	0.554
	$6s+6p$	0.128	0.154
	$6d+6f+6g+6h$	0.205	0.257
	$\boldsymbol{n=6}$	0.333	0.412
	$\boldsymbol{n=7}$	0.017	0.034
0.75	$\boldsymbol{n=4}$	0.058	0.068
	$5s$	0.042	0.044
	$5p$	0.105	0.074
	$5d+5f+5g$	0.373	0.334
	$\boldsymbol{n=5}$	0.520	0.452
	$6s+6p$	0.041	0.021
	$6d+6f+6g+6h$	0.336	0.382
	$\boldsymbol{n=6}$	0.377	0.403
	$\boldsymbol{n=7}$	0.055	0.076

followed very slightly different trajectories to the detectors due to the unscreened earth's magnetic field, and a direct calibration for each ion separately was the most reliable approach.

The experimental Q-value spectra for atomic hydrogen targets are shown in Figs. 5–7 (O^{8+}) and Figs. 8–10 (Ar^{8+}). By integrating the peaks in the experimental spectra, relative partial capture cross sections into different n states of O^{7+} and different n,l states for Ar^{8+} can be obtained. These are shown and compared to the theoretical results in Tables I and II. The agreement between theory and experiment is excellent. It might be expected on the basis of the molecular potential curves in Figs. 3 and 4 that the $n=6$ crossing would be too far out (around 15–20 a.u.) to be active and that only $n=5$ would be appreciably populated. Such an assumption has been made in previous calculations. The data clearly show this not to be the case, and the theoretical calculation is in good agreement on this point. As v is raised, the major effects seen are a broadening of the Q window and a tendency for higher l values (for the Ar^{8+} case) to be more strongly populated. This is seen in both the experiment and the theory.

TABLE II. Same as Table I but for $O^{8+}+H(1s)$.

v (a.u.)	σ_n	AOCC	Expt.
0.5	$n=4$	0080	0.048
	$n=5$	0.634	0.634
	$n=6$	0.275	0.281
	$n=7$	0.011	0.037
0.75	$n=4$	0.107	0.073
	$n=5$	0.593	0.498
	$n=6$	0.281	0.364
	$n=7$	0.019	0.065
0.95	$n=4$	0.140	0.098
	$n=5$	0.539	0.405
	$n=6$	0.283	0.365
	$n=7$	0.038	0.132

Since capture data from molecular hydrogen is also present in our data, we show in Figs. 11–14, Q-value spectra for the molecular target. In Fig. 11 the comparison is made by plotting data from the two targets on the same plot. Since the vertical ionization energy for molecular hydrogen is 16.3 eV, 2.7 eV more than that for atomic hydrogen, one would expect to see the H_2 spectrum shifted by 2.7 eV toward larger Q values. This is seen to be approximately the case. A slightly different n distribution is also perhaps present, since the Q window does not shift. A more interesting effect is the clear broadening of the peaks for the hydrogen target. This is unlikely to be due to experimental effects, since the two data sets were taken simultaneously under identical conditions. Such an effect would be expected if a slight vibrational excitation of the H_2^+ target were to accompany the capture. Such an effect should also shift the molecular Q-value spectrum slightly to smaller Q values, but our uncertainty in the relative positions of the Q-value scales for the two different recoil ions prevents our evaluation of this effect. For the case of Ar^{8+}, a similar broadening is seen for the molecular target and observable changes in the population distributions are seen which we attribute to the slight shift in position of the Q window. The Q-value distributions we measure for $v=0.32$ a.u. are in good agreement with those reported by Boudjema *et al.* [35] for metastable Ar^{8+} projectiles on molecular deuterium, and with the multichannel Landau-Zener calculations presented there. We note that if sufficient excitation, either vibrational or electronic, is imparted to the molecular hydrogen target, dissociative capture may result, and the corresponding channel would escape our detection in the present experiment. Since the observed vibrational excitation is, at best, weak, dissociative capture through ground-state dissociation is unlikely to be strong in this case. It is possible that electronically excited potential curves of the hydrogen could be populated, but electronic excitation of the target accompanying single electron capture is known to be weak in situations such as this. In any event, our data have nothing to say about this issue.

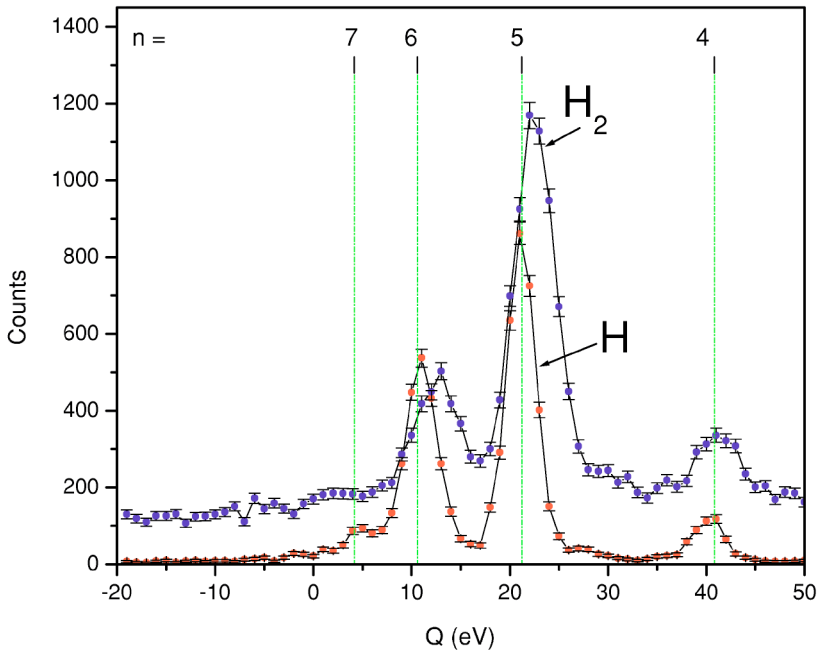

FIG. 11. (Color online) Comparison of Q-value spectra for capture from atomic and molecular hydrogen by O^{8+} ions at $v=0.75$ a.u. The location of the expected Q values for capture to different n levels of O^{7+} are indicated for the atomic hydrogen case.

A recurring theme in the discussion of low energy capture by projectiles such as Ar^{8+} is the possibility of a metastable beam component. While it is well known that Ar^{8+} beams do often have metastables present, this is much less a problem with an electron beam ion source (EBIS) than with other sources because the cycle time is tens of milliseconds, thus giving the metastables a long average relaxation time. In addition, the electron energy in an EBIS is controlled at a low value. There is no evidence for metastable beams in any or our previous work with He targets [6–12].

Finally in Fig. 15 we show the distribution of the transverse momentum transfer for capture from atomic hydrogen

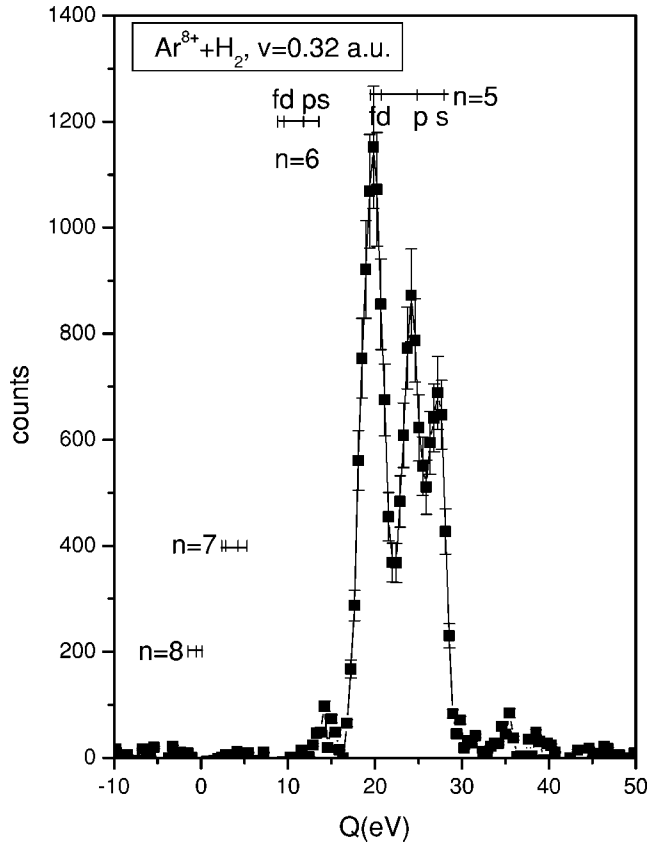

FIG. 12. Similar to Fig. 8, but for a molecular target.

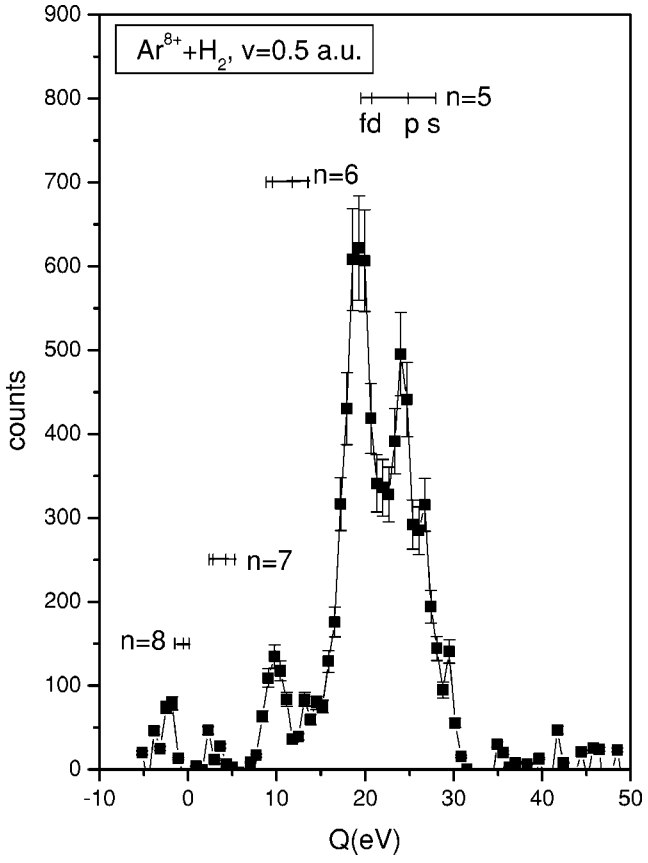

FIG. 13. Similar to Fig. 12, but for $v=0.75$ a.u.

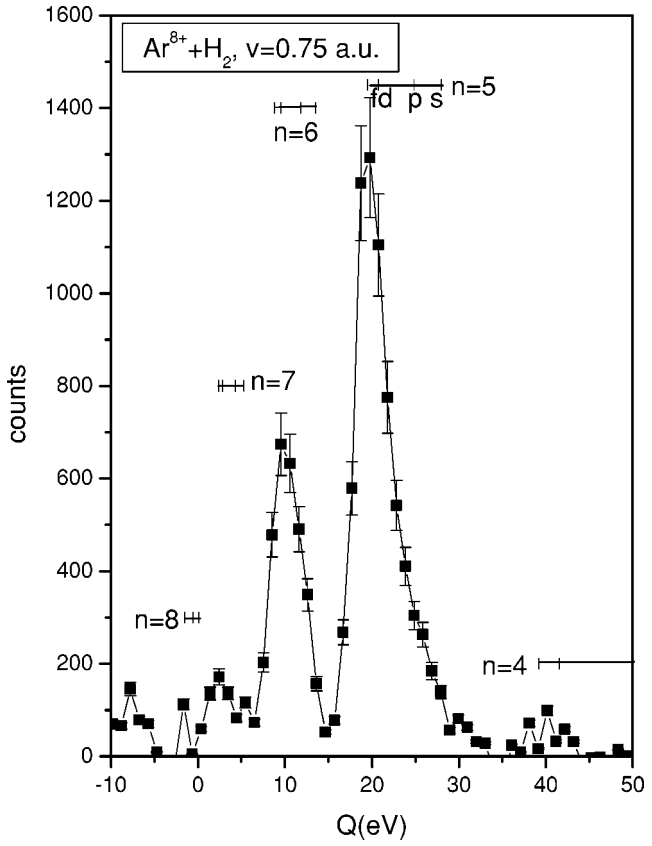

FIG. 14. Similar to Fig. 12, but for $v=0.75$ a.u.

for O^{8+} at $v=0.75$ a.u., which is typical for all cases studied in this paper. As discussed in previous papers on this subject, if capture were to take place only at an impact parameter equal to the crossing radius for population of a channel corresponding to a certain Q value, the scattering angle θ_c which would result from the outgoing Coulomb trajectory of the projectile would be given by the simple expression $\theta_c = E/2Q$, where E is the laboratory projectile energy. In the language of transverse momentum transfer, P_{trans}, rather than scattering angle, this expression is, $P_{\text{trans}} = mQ/p_o$, where m and p_o are the projectile mass and laboratory momentum, respectively. We show this relationship as a dashed line in Fig. 15. One generally expects that the transverse momentum transfer is spread on both sides of this line, due to capture on the way in and way out, and this is indeed seen to be the case. It is clear that no localization of capture along this line occurs for such fast collisions, and that a full treatment of the quantal nature of the collisions would be necessary to describe the experimental scattering distribution. On the basis of previous results from the TCAOCC calculation, we expect that the present theoretical treatment would be able to do this [12].

V. SUMMARY

We have presented experimental Q-value spectra for the capture from atomic and molecular hydrogen by O^{8+} and Ar^{8+} ions, and have deduced relative partial capture cross sections for capture into different n and (n,l) final states of the resulting 7+ ions, respectively. We have covered a velocity range from 0.32 to 0.96 a.u., over which the spreading of the Q window is observed as well as a tendency for higher l states to be populated for higher v. We have carried out two

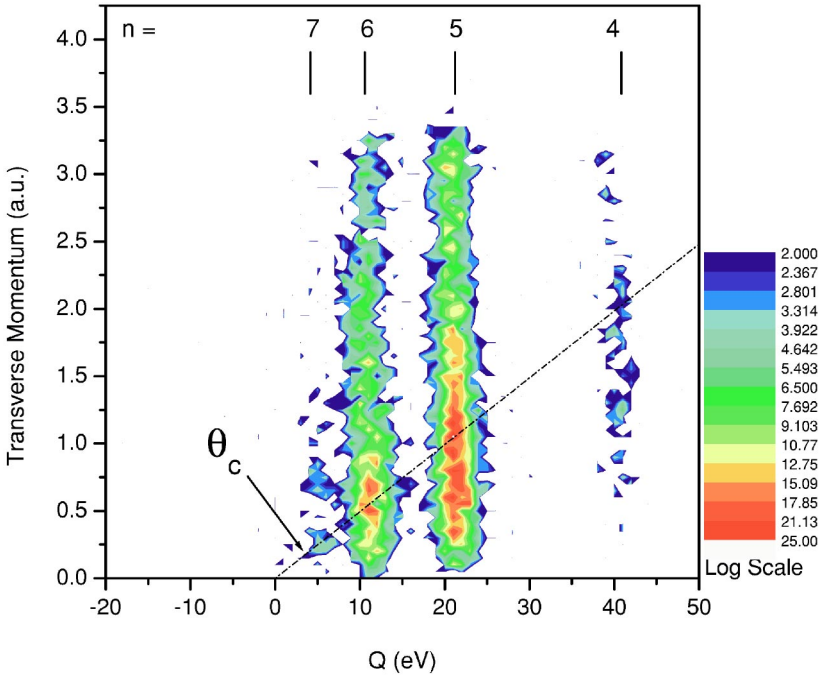

FIG. 15. (Color online) Density plot of transverse vs longitudinal momentum transfer for capture from atomic hydrogen by O^{8+} at $v=0.75$ a.u. The dashed line shows the locus of expected transverse momentum transfer for a capture taking place at the crossing radius.

center atomic orbital close coupling calculations for the atomic targets for both projectiles. Excellent agreement between experiment and theory is found. To all indications, electron capture by highly charged projectiles is under very good theoretical control over this range of collision velocities.

ACKNOWLEDGMENTS

This work was supported by the Chemical Sciences, Geosciences and Biosciences Division of the Office of Basic Energy Sciences, Office of Science, U. S. Department of Energy.

[1] M. Barat and P. Roncin, J. Phys. B **25**, 2205 (1992).
[2] E. K. Janev and H. Winter, Phys. Rep. **117**, 265 (1985).
[3] E. K. Janev and L. P. Presnyakov, Phys. Rep. **70**, 1 (1981).
[4] C. L. Cocke, in *Review of Fundamental Processes and Applications of Atoms and Ions*, edited by C. D. Lin (World Scientific, Singapore, 1993), p. 111.
[5] A. Niehaus, J. Phys. B **19**, 2925 (1986).
[6] J. Ullrich *et al.*, Comments At. Mol. Phys. **30**, 285 (1994).
[7] R. Doerner *et al.*, Phys. Rep. **330**, 95 (2000).
[8] M. A. Abdallah, W. Wolff, H. E. Wolf, E. Y. Kamber, M. Stockli, and C. L. Cocke, Phys. Rev. A **58**, 2911 (1998).
[9] V. Mergel *et al.*, Phys. Rev. Lett. **79**, 387 (1997).
[10] A. Cassimi *et al.*, Phys. Rev. Lett. **76**, 3679 (1996).
[11] X. Flechard, S. Duponchel, L. Adoui, A. Cassimi, P. Roncin, and D. Hennecart, J. Phys. B **30**, 3697 (1997).
[12] M. A. Abdallah, W. Wolff, H. E. Wolf, E. Sidky, E. Y. Kamber, M. Stockli, C. D. Lin, and C. L. Cocke, Phys. Rev. A **57**, 4373 (1998).
[13] B. H. Bransden and M. R. C. McDowell, *Charge Exchange and Theory of Ion-Atom Collisions*, The International Series of Monographs on Physics Vol. 82 (Clarendon Press, Oxford, 1992).
[14] W. Fritsch and C. D. Lin, Phys. Rep. **202**, 1 (1991).
[15] Jiyun Kuang and C. D. Lin, J. Phys. B **29**, 1207 (1996).
[16] T. G. Lee, H. Nguyen, X. Flechard, B. D. DePaola, and C. D. Lin, Phys. Rev. A **66**, 042701 (2002).
[17] D. H. Crandall, R. A. Phaneuf, and F. W. Meyer, Phys. Rev. A **22**, 379 (1980); **19**, 504 (1979).
[18] F. W. Meyer, A. M. Howald, C. C. Havener, and R. A. Phaneuf, Phys. Rev. A **32**, 3310 (1985).
[19] C. Can, T. J. Gray, S. L. Varghese, J. M. Hall, and L. N. Tunnell, Phys. Rev. A **31**, 72 (1985).
[20] D. Dijkkamp, D. Ciric, and F. J. deHeer, Phys. Rev. Lett. **54**, 1004 (1985).
[21] R. Hoekstra, D. Ciric, F. J. deHeer, and R. Morgernstern, Phys. Scr., T **28**, 81 (1989).
[22] R. Hoekstra, D. Ciric, F. J. deHeer, and R. Morgernstern, Phys. Lett. A **124**, 73 (1987).
[23] R. Hoekstra, Ph.D dissertation, University Groningen (unpublished).
[24] J. P. Giese, C. L. Cocke, W. Waggoner, L. N. Tunnell, and S. L. Varghese, Phys. Rev. A **34**, 3770 (1986).
[25] D. M. Kearns, R. W. McCullough,R. Trassel, and H. B. Gilbody, J. Phys. B **36**, 3653 (2003).
[26] A. Salop and R. E. Olson, Phys. Rev. A **13**, 1312 (1976).
[27] E. J. Shipsey, T. A. Green, and J. C. Browne, Phys. Rev. A **27**, 821 (1983).
[28] R. K. Janev, D. S. Belic, and B. H. Bransden, Phys. Rev. A **28**, 1293 (1983).
[29] H. Knudsen, H. K. Haugen, and P. Hvelplund, Phys. Rev. A **24**, 2287 (1981).
[30] W. Fritsch and C. D. Lin, Phys. Rev. A **29**, 3039 (1984).
[31] W. Fritsch, Phys. Rev. A **30**, 3324 (1984).
[32] J. P. Hansen and K. Taulbjerg, Phys. Rev. A **40**, 4082 (1989).
[33] B. P. Paolini and M. A. Khakoo, Rev. Sci. Instrum. **69**, 3132 (1998).
[34] See http://physics.nist.gov/cgi-bin/AtData/levels_form
[35] M. Boudjema, A. Benoit-Catlin, A. Bordenave-Montesquieu, and A. Gleizes, J. Phys. B **21**, 103 (1988).